Natural Rubber Nanocomposites with Functionalized Carbon Nanotubes: Mechanical, Dynamic Mechanical, and Morphology Studies

Adedigba A. Abdullateef,[1] Selvin P. Thomas,[1] Mamdouh A. Al-Harthi,[1,2] S. K. De,[1] Sri Bandyopadhyay,[3] A. A. Basfar,[4] Muataz A. Atieh[1,2]

[1]*Department of Chemical Engineering, King Fahd University of Petroleum and Minerals, Dhahran 31261, Kingdom of Saudi Arabia*
[2]*Center of Research Excellence in Nanotechnology (CENT), King Fahd University of Petroleum and Minerals, Dhahran 31261, Kingdom of Saudi Arabia*
[3]*School of Materials Science and Engineering, University of New South Wales, Sydney 2052, Australia*
[4]*Atomic Energy Research Institute, King Abdulaziz City for Science and Technology, Riyadh 11442, Kingdom of Saudi Arabia*

Received 18 October 2010; accepted 27 May 2011
DOI 10.1002/app.35021
Published online 27 December 2011 in Wiley Online Library (wileyonlinelibrary.com).

ABSTRACT: Recent attempts toward improving the properties of natural rubber (NR) by using carbon nanotubes (CNT) as filler were not successful due to low dispersion of CNT in NR. This article reports the results of studies on improvement of dispersion of CNT in NR by acid modification of CNT surface. Fourier transform infrared spectra confirmed the presence of COOH groups on the CNT surface. On the basis of results of studies on using differential scanning calorimetry, universal testing machine, dynamic mechanical tester, thermogravimetric analysis, electrical properties, and transmission electron microscopy, it is concluded that acid modification of CNT leads to improvement in thermal stability, stress–strain, and dynamic mechanical properties. © 2011 Wiley Periodicals, Inc. J Appl Polym Sci 125: E76–E84, 2012

Key words: natural rubber; carbon nanotubes; functionalization; dynamic mechanical properties; crystallization

INTRODUCTION

Natural rubber (NR) exhibits outstanding properties such as green strength and tensile strength because it can crystallize spontaneously when it is strained. However, a few properties of NR such as modulus, hardness, and abrasion resistance need to be improved for specific applications. Carbon black (CB) and silica are the conventional reinforcing fillers used to enhance the mechanical properties of various rubbers. However, the modulus and durability of a neat rubber is low, and addition of reinforcing agents is essential for practical applications. Since high loadings of CB or silica are necessary to achieve the reinforcement in rubber, it is anticipated that the mechanical and physical properties of a rubber may be improved through the addition of a low amount of nanoscale fillers due to the higher specific surface area.[1–4]

Short fibers and whiskers are also known to act as reinforcers in rubbers.[5,6] Recently, carbon nanotubes (CNT) have been reported to act as reinforcing fillers for different polymer matrices.[7–9] Of late, CNT has evoked interest as filler in NR due to their outstanding physical and mechanical characteristics.[10–13] There are reports of studies on nanofiller-reinforced rubber, but the dispersion of CNT into rubbers needs greater attention due to high aspect ratio of the CNT and high viscosity of rubber.[14–16] Methods to achieve improvement in the homogenous dispersion of CNT in the polymer matrix include use of dispersion aids or surface active agents and chemical functionalization of the CNT surface.[9,17]

This article reports the results of studies on the effects of surface oxidized CNT on mechanical and dynamic mechanical properties of NR.

EXPERIMENTAL

Materials

NR used in this experiment is ribbed smoked sheet NR (RSS1) obtained from Amiantit Rubber

Correspondence to: Dr. M. A. Atieh (motazali@kfupm.edu.sa) or Prof. S. K. De (sadhan@kfupm.edu.sa).

Contract grant sponsor: King Abdulaziz City for Science and Technology (KACST) through Science and Technology Unit at King Fahd University of petroleum and Minerals (KFUPM); contract grant number: 09-ADV789-04.
Contract grant sponsor: National Science, Technology, and Innovation Plan.

TABLE I
Vulcanization Recipe for the Composites

Component	Composition (phr)[a]
NR	100
CNT	0, 1, 5, and 10
Sundex oil[b]	10
ZnO[c]	4.8
Stearic acid	2.0
IPPD[d]	1.0
TMQ[e]	2.0
Wax	1.0
TMTD[f]	1.5
MBT[g]	0.5
Sulfur	0.4

[a] phr stands for parts per hundred parts rubber by weight.
[b] Processing oil.
[c] Zinc oxide (activator).
[d] N-Isopropyl-N′-phenyl-paraphenylenediamine (antioxidant).
[e] 2,2,4-Trimethyl-1,2-dihydroquinoline (antioxidant).
[f] Tetramethyl thiuram disulfide (accelerator).
[g] 2-Mercaptobenzothiazole (accelerator).

Industries, Saudi Arabia. Ribbed smoked sheet (RSS) refers to rubber sheets that are transformed from liquid fresh latex to solid rubber sheets by adding formic acid, and consecutive smoke drying at 50–60°C to preserve the quality of the rubber. Smoked sheets are categorized to different grades (RSS1–RSS5) based on their quality, color, and contaminations. The characteristics of the used rubber are dirt content of 0.04% by mass, volatile matter of 0.50% by mass, ash content of 0.40% by mass, initial plasticity of 40, and plasticity retention index of 78. The multi walled CNT were purchased from Nanostructured and Amorphous Materials, Inc. (Houston, TX). The Purity of CNT is >95%, its outside and inside diameters are 20–40 nm and 10–20 nm, respectively. The length of these CNTs is 10–30 μm. Toluene used was of analytical grade purchased from Sigma Aldrich. Nitric acid (69–71% purity) was used to treat the as received CNT.

Acid modification of CNT

The modification with concentrated nitric acid was done to impart —COOH groups on the surface of CNT. One gram of the CNT was modified with 10 mL of concentrated nitric acid at a temperature of 120°C for 48 h under continuous stirring using a magnetic stirrer.[9,17] Then it was washed with deionized water to remove excess nitric acid. The acid modified CNT is henceforth designated as *m*-CNT.

Composite preparation

The composites were prepared by dissolving 25 g of NR in 1000 mL of toluene. The CNT was sonicated for 30 min to reduce the agglomeration of the nanotubes and was added to the rubber solution in concentrations of 1, 5, 10 g per 100 g of rubber (phr). The NR/CNT mixture was mechanically stirred for 20 min for obtaining a uniform dispersion and then dried in open air at room temperature. NR/CNT compositions as prepared above were compounded using the standard vulcanization recipe (Table I). The compounding was performed at 80°C for 15 min in a two roll mill. Cross-linking or curing of the compounded samples was carried out in a hot press at 150°C for 30 min.

Characterization techniques

The CNT was characterized by field emission scanning electron microscopy (FE-SEM) (JEOL JSM-6700F) and transmission electron microscopy (TEM; Philips CM200-FEG). To prepare TEM samples, some alcohol was dropped on the nanotubes film,

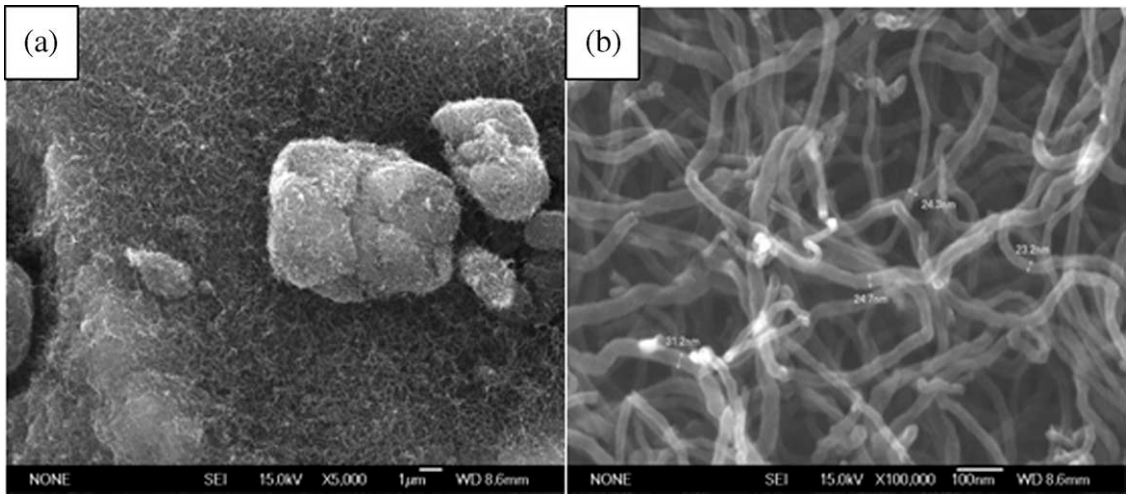

Figure 1 SEM Images of carbon nanotubes at (a) at low resolution (b) at high resolution.

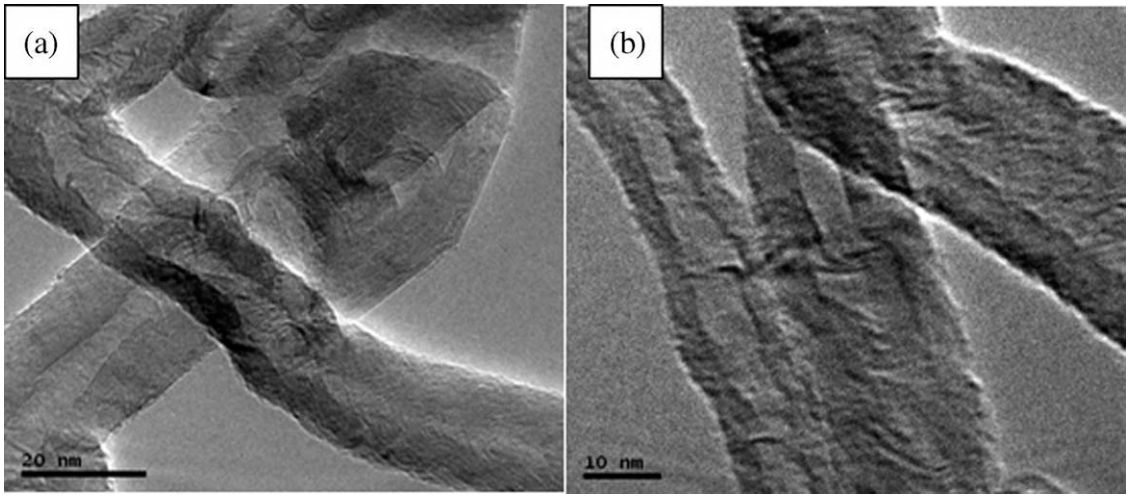

Figure 2 TEM Images of carbon nanotubes (a) at low resolution (b) at high resolution.

and then these films were transferred with a pair of tweezers to a carbon-coated copper grid. Both the unmodified CNT and CNT-COOH was characterized using Fourier transform infrared spectroscopy (Perkin–Elmer 16F PC FTIR) instrument. FTIR samples were prepared by grinding dried functionalized CNT together with potassium bromide (KBr) to make a pellet. The thermal property of the composite produced was tested using differential scanning calorimetry with robotic arm (DSC-Q1000) from TA instrument. Samples weight used ranges from 7 to 9 mg which were sealed in aluminum nonhermetic pans. The measurements were obtained in the temperature range of −80 to 100°C at heating rate of 10°C/min under nitrogen environment with flow rate of 50 mL/min. The obtained data were analyzed using the universal analysis 2000 from TA instrument. Tensile tests were carried out on the samples using Zwick tensile testing machine with specimen grip of 50 mm and testing speed of 500 mm/min. Five specimens each 35 mm in length and 2 mm in thickness were prepared from each batch and tested according to ASTM D412. Dynamic mechanical tests were conducted in tension mode using DMA Q800 (TA instruments) with liquid nitrogen attachment from −120 to 100°C at a frequency of 1 Hz and an amplitude of 10 μm. Philips CM200 TEM was used with a field emission gun (FEG), which provides very high resolution for the TEM measurements under high vacuum. The samples were prepared using a Leica FC6 Cryo-ultramicrotome. A small piece of the sample was mounted in cellulose and was cut into slices of 60 nm thickness by a diamond knife.

The DC volume resistivity of the composite materials having wide range of resistivity were measured using instruments Agilent 4339B (high resistance meter attached with Agilent 16008B resistivity cell) [measurement range covering from 10^{16} ohm to 10^{6} ohm] and GOM-802 (GW Instek DC milli Ohm Meter) for low resistance measurement. GOM-802 is remaining attached with a home-made electrode and covering range from 10^{6} ohm to 10^{-3} ohm.

RESULTS AND DISCUSSION

Characterization of CNT

The CNT were characterized by using FE-SEM and TEM. The outside diameter of the CNT varied from 20 to 40 nm with average diameter at 24 nm while the length of the CNTs was up to few microns. Figure 1(a) shows the SEM image of CNT at low magnification and Figure 1(b) shows the same at high magnification. TEM was carried out to characterize the structure of nanotubes [Fig. 2(a,b)]. It is obvious from the images that all the nanotubes are hollow and tubular in shape. In some of the images, catalyst particles can be seen inside the nanotubes. TEM

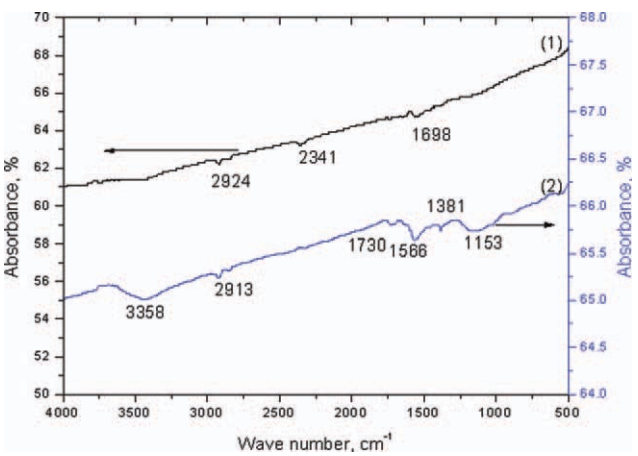

Figure 3 FTIR spectra of (1) unmodified CNT and (2) acid-modified CNT (*m*-CNT) indicating presence of carbonyl and hydroxyl groups. [Color figure can be viewed in the online issue, which is available at wileyonlinelibrary.com.]

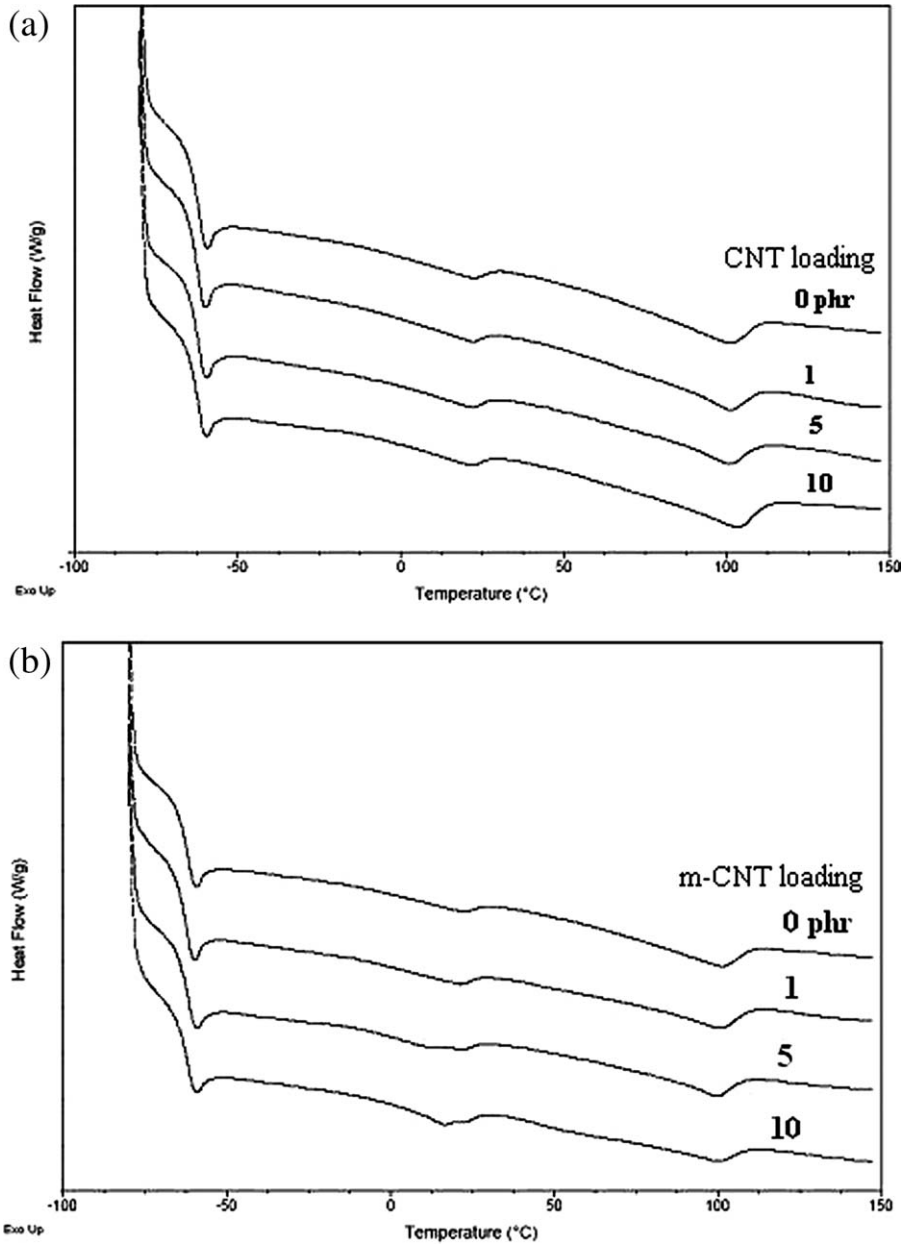

Figure 4 DSC thermograms of NR/CNT composites (a) unmodified CNT and (b) *m*-CNT.

images indicate that the nanotubes have uniform diameter distribution and contain no deformity in the structure. Figure 2(b) shows the high resolution transmission electron microscope (HRTEM) of the CNT wherein highly ordered crystalline structure is present.

TABLE II
Results of DSC Studies of NR-CNT Composites[a]

Concentration of CNT (phr)	T_g (°C)		T_{m1} (°C)		ΔH_{m1} (J/g)		χ_{c1} (%)		T_{m2} (°C)		ΔH_{m2} (J/g)		χ_{c2} (%)	
	CNT	*m*-CNT	CNT	*m*-CNT	CNT	*m*-CNT	CNT	*m*-CNT	CNT	*m*-CNT	CNT	*m*-CNT	CNT	*m*-CNT
0	−61.7	−61.7	22.8	22.8	0.275	0.275	0.18	0.18	101.7	101.7	0.854	0.854	0.59	0.59
1	−61.9	−61.8	21.7	21.9	0.303	0.585	0.45	0.45	101.2	101.8	1.065	1.234	0.77	0.83
5	−61.7	−61.7	21.9	21.8	0.31	0.602	0.46	0.48	101.3	101.8	1.074	1.358	0.82	0.97
10	−62.1	−62.1	21.9	21.2	0.315	0.635	0.48	0.51	103.5	102.9	1.465	2.128	1.09	1.56

[a] *m*-CNT stands for acid modified CNT.

TABLE III
Mechanical Properties of NR-CNT Composites[a]

CNT loading (phr)	Tensile strength (MPa)		Modulus (MPa)		Elongation (%)		Toughness (J/m^3)	
	CNT	*m*-CNT	CNT	*m*-CNT	CNT	*m*-CNT	CNT	*m*-CNT
0	15.0	15.0	0.53	0.53	1332	1332	62.5	62.5
1	18.5	18.9	0.65	0.67	1316	926	77.7	60.3
5	17.8	18.7	1.02	0.98	948	714	60.0	57.1
10	15.4	15.1	1.12	1.26	727	569	48.3	31.2

[a] *m*-CNT stands for surface modified CNT.

FTIR analysis

The FTIR spectra for the unmodified CNT and acid modified CNT, designated as *m*-CNT, are shown in Figure 3. The unmodified CNT show only a few weak peaks in the spectra, especially corresponding to the OH groups and C=O groups due to the absorption of water molecules and oxidation of the carbon chains. But the spectra of the *m*-CNT shows that the peak attributed to C=O shows increased intensity in the region 1698 cm^{-1} which confirms the oxidation of the CNT surface. The peaks in the region of 3398 and 3797 cm^{-1} are due to the presence of hydroxyl groups.[13,18–20] Furthermore, there are peaks corresponding to the C—O—C stretching in the 1000–1100 cm^{-1} region.

DSC measurements

The DSC studies were undertaken to study the effect of CNT and *m*-CNT on the glass transition temperature as well as the crystallization temperature of the NR composites. Figure 4 shows the DSC heating curves of the composites with unmodified as well as acid modified CNT. It is to be noted that the T_g of NR, around −61.72°C, does not show significant changes in both CNT and *m*-CNT composites. Small shifting by 1–3°C to higher temperature is due to the filler effect on incorporation CNT into the composites.

The DSC measurements, however, showed an interesting observation in the crystallization of NR. As can be seen from Figure 4, all the composites show two distinct melting peaks around 20°C and 101°C. It is believed that two types of rubber crystallites were formed in the composites. In the first case of low temperature melting zone, the rubber chains coil over the CNTs to form an ordered form and in the second case of high temperature melting zone these ordered coils become associates during the subsequent vulcanization process. Therefore, two different melting zones are shown in the DSC thermograms. However, the amount of crystallinity is very small, as is evident from the percentage crystallinity values (Table II). It can also be seen that the peak area increases as the CNT loading increases. Further studies are in progress to elucidate the exact mechanism of the crystallization phenomenon. Thus, it can be concluded that the incorporation of CNT helps crystallization of NR by coiling of the rubber chains over the CNT surface. The effect of surface modified CNT on crystallization behavior of NR is shown in Table II. Although there is insignificant change in the case of low temperature melting, the high temperature melting peak temperature shifts to

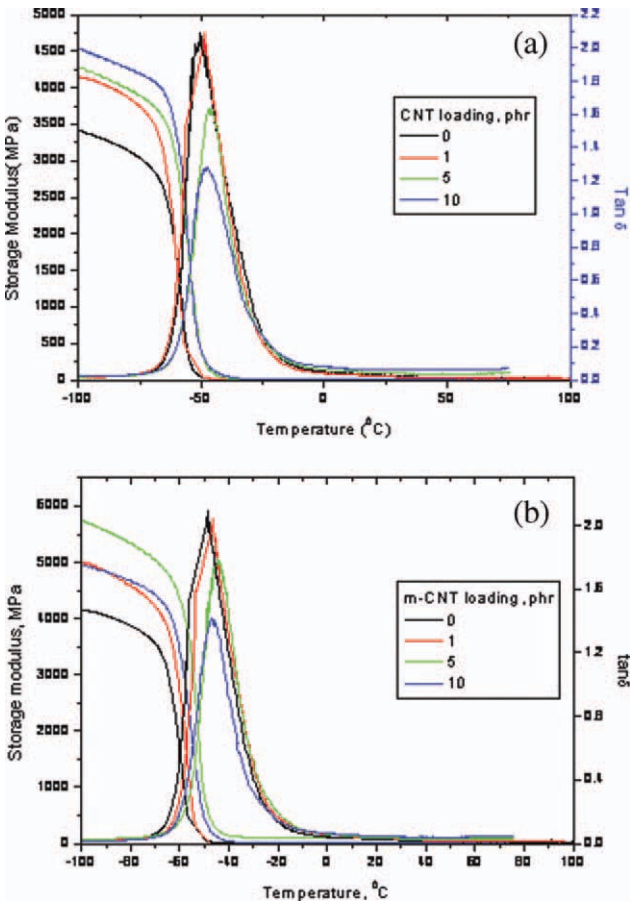

Figure 5 Storage modulus and tan δ curves of NR/CNT composites with (a) unmodified and (b) modified CNT. [Color figure can be viewed in the online issue, which is available at wileyonlinelibrary.com.]

TABLE IV
Storage Modulus, Loss Modulus, and Glass Transition Temperature of the NR-CNT Composites[a]

	−100°C		−50°C		−25°C		0°C		25°C	
CNT loading	CNT	*m*-CNT	CNT	*m*-CNT	CNT	*m*-CNT	CNT	*m*-CNT	CNT	*m*-CNT
(a) Storage moduli (MPa) at different temperatures										
0	3863	3863	89.9	81.2	21.7	162.5	15.8	170.6	15.3	179.8
1	4160	5030	47.6	184.6	19.8	160.4	15.8	170.5	15.3	179.9
5	4270	5741	401.1	730.1	20.7	150.4	15.9	170.5	15.3	179.9
10	4523	4954	397.6	463.1	20.6	130.1	16.0	170.4	15.3	180.0
(b) Loss moduli (MPa) at different temperatures										
0	66	66	140.1	160.4	0.2	0.6	0.05	0.08	0.01	0.05
1	75	99	98.7	165.3	0.6	0.9	0.1	0.1	0.1	0.07
5	86	156	537.4	319.7	1.6	1.7	0.3	0.3	0.2	0.2
10	106	118	488.5	555.8	3.6	2.7	0.7	0.5	0.7	0.3

higher temperature, suggesting association of stronger crystallites in the presence of modified CNT.

Mechanical properties

From the stress–strain curves, tensile strength, Young's modulus, elongation at break and toughness were calculated (Table III). The tensile strength of the composites shows an increase on incorporation of 1 phr of CNT, while higher loading of CNT causes a decrease in tensile strength. Filler effect causes increase in Young's modulus of the composites, while the elongation at break and toughness decrease at higher filler loading. Acid modification of CNT causes no significant changes in modulus and tensile properties, while the elongation at break and toughness show a decrease. Similar results were reported by Sui et al. while studying modified CNT reinforced NR matrix.[15] Since NR itself has high strength due to its strain crystallization behavior, incorporation of reinforcing fillers causes insignificant changes in the tensile strength of NR vulcanizates.[21,22]

Dynamic mechanical analysis

Dynamic mechanical properties of the composites were measured to study the effect of CNT on the storage modulus, loss modulus, and tan δ of NR from −100 to 150°C. Figure 5 shows the variation in storage modulus and tan δ of the composites of both unmodified and acid modified CNTs. It can be seen that the storage modulus values show a sharp decrease around −50°C which happens to be the glass transition temperature of NR in the composites. The curves show three distinct regions, the

TABLE V
Glass Transition Temperature from $(\tan \delta)_{max}$ and (loss modulus)$_{max}$

	Tan δ (°C)		*E″* (°C)	
CNT loading	CNT	*m*-CNT	CNT	*m*-CNT
0	−48.9	−48.8	−59.7	−59.7
1	−50.3	−46.6	−59.3	−56.7
5	−46.1	−44.4	−54.7	−53.2
10	−47.8	−44.5	−55.1	−55.6

[a] *m*-CNT stands for modified CNT.

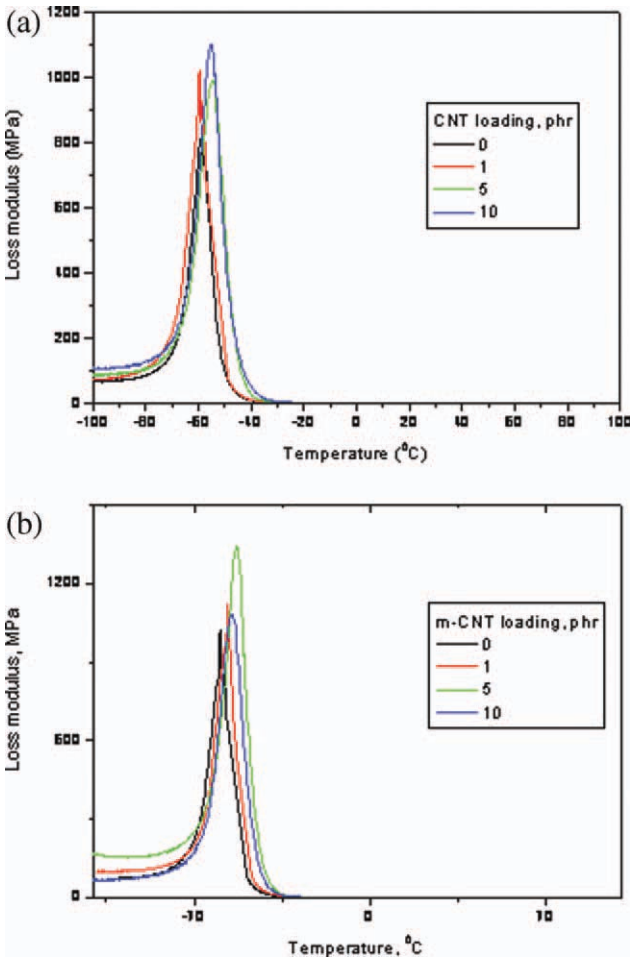

Figure 6 Loss modulus curves of NR/CNT composites with (a) unmodified and (b) modified CNT. [Color figure can be viewed in the online issue, which is available at wileyonlinelibrary.com.]

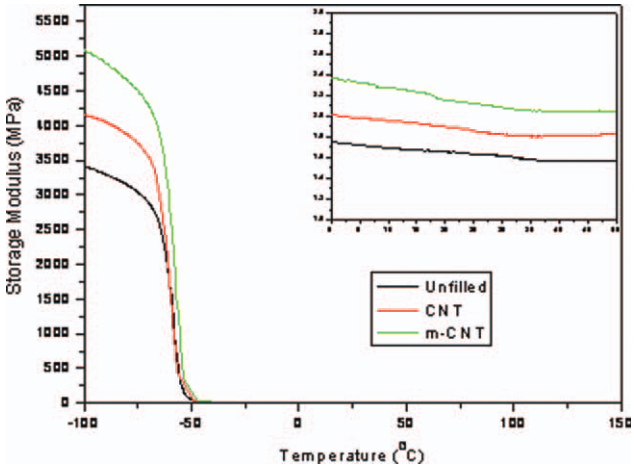

Figure 7 Storage modulus versus temperature plots of unfilled and filled NR/CNT composites at 1% filler loading. Inset shows the variation in the room temperature region. [Color figure can be viewed in the online issue, which is available at wileyonlinelibrary.com.]

glassy state, glass to rubber transition region, and the rubbery state. The storage modulus values are constant before the glass transition. The variation of storage modulus at different temperatures is given in Tables IV and V. It is evident that the increase in CNT loading causes many-fold increase in the storage modulus in the glassy region which can be attributed to the good matrix–filler interaction. The increase in test temperature decreases the storage modulus and beyond the glass transition temperature, the storage modulus values are almost constant. In the transition temperature zone between −25°C to −50°C, the rubber is in a leathery state and the behavior in the leathery state is different from that in glassy state (−100°C) and in the rubbery

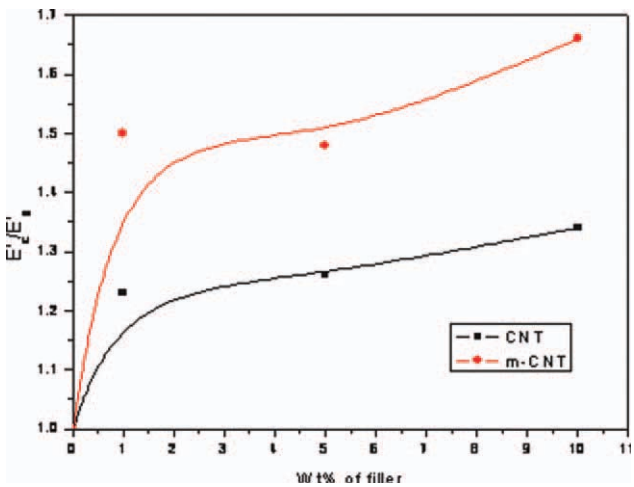

Figure 8 Plots of $E'c/E'g$ at −100°C versus filler loading; $E'c$ and $E'g$ stand for storage modulus for CNT-filled NR and unfilled (gum) NR, respectively. [Color figure can be viewed in the online issue, which is available at wileyonlinelibrary.com.]

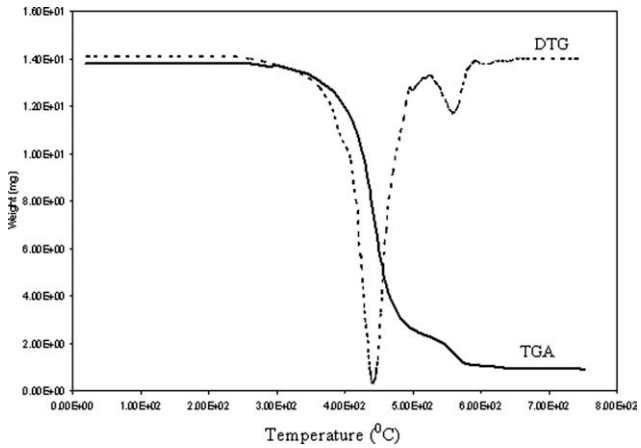

Figure 9 Representative TGA and DTG curves of NR/CNT composites.

state (0 and 25°C). Accordingly, this anomalous behavior at −25°C and to some extent at −50°C can be assigned to the leathery behavior in the region, which needs further investigation.

The loss modulus curves of the composites with unmodified and acid-modified CNT are given in Figure 6. All the curves show similar behavior typical for rubber composites and show a peak maximum corresponding to the glass transition temperature around −50°C. The variation of loss modulus at different temperatures is given in Tables IV and V. The composites with acid-modified CNTs show higher loss modulus at all temperatures indicating good interaction with NR matrix.

The variation in storage modulus with respect to filler loading is represented in Figure 7. There is many-fold increase in storage modulus in the low temperature region. The addition of CNT into NR matrix causes significant improvement in the storage modulus indicating good interaction between the matrix and CNT. The composites with modified CNT also shows good enhancement in storage modulus. It is believed that the surface modification of CNT enhanced the filler dispersion into the NR matrix. The variation of storage modulus around room temperature is shown in the inset in Figure 8. Here also the trend continues, however, the magnitude of increase is small.

The variation of the ratio of storage modulus of the composites to the storage modulus of the gum rubber (unfilled) with respect to the filler loading at −100°C is given in Figure 8. The ratio increases with increase in CNT loading and the effect is pronounced in the case of surface modified CNT, presumably due to improved filler dispersion and consequently higher filler–matrix interaction.

The effect of CNT loading on the glass transition is evident from the tan δ and the loss modulus curves. Tables IV and V summarizes the glass transition temperature values obtained from loss modulus

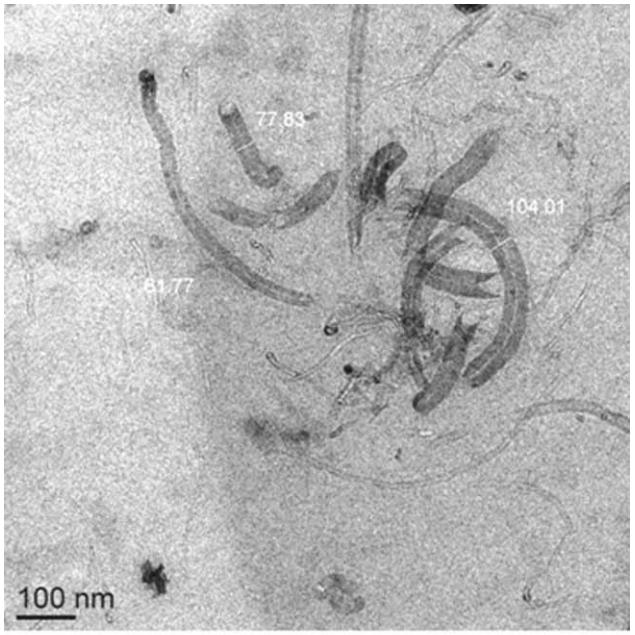

(a)

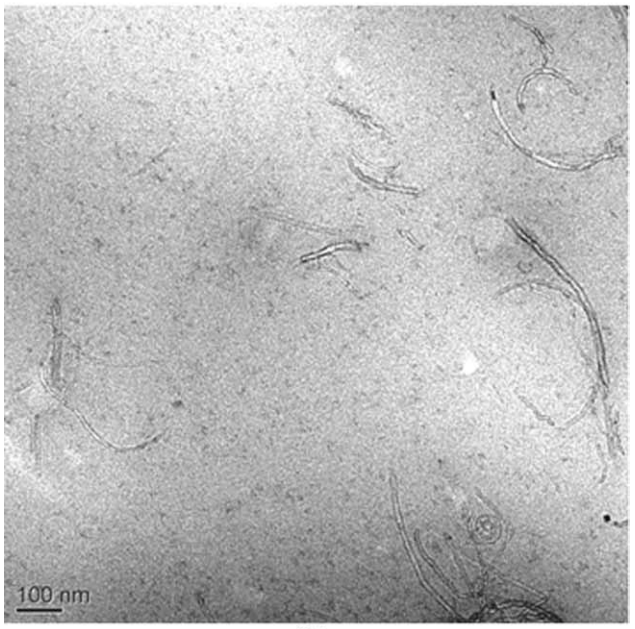

(b)

Figure 10 TEM images composites at 1% filler loading (a) NR/CNT and (b) NR/*m*-CNT.

curves and tan δ. As expected, the T_g values are lower for the loss modulus compared with the tan δ. The acid modification of the CNT shows an increase in T_g for all loadings, and the tan δ values decrease with respect to filler loading, indicating good filler–matrix interaction.

Thermogravimetric analysis

Figure 9 shows the representative thermogram of the NR composites. As can be seen from the DTG curves, the composites show two distinct degradation steps. The first one around 440°C is the major degradation step for all the composites. The addition of CNT does not improve the thermal stability to a great extent. The acid-modified CNTs, however, showed improvement in the thermal stability by increasing the degradation temperature by almost 10°C.

Electron microscopy

TEM images of the 1% filled composites are given in Figure 10. Although the unmodified CNT filled composites show individual CNTs in the matrix, a few loose agglomerates can be seen. The TEM image of composite with modified CNT shows good dispersion of individual nanotubes in the matrix. Thus, it can be concluded that the acid modification of the nanotubes enables the higher degree of dispersion in the NR matrix.

Electrical properties

Volume resistivity decreases on incorporation of CNT as shown in Figure 11. After functionalization, better dispersion as well as presence of surface-COOH groups cause increase in resistivity. Similar observations have been made while measuring CB dispersions in rubbery matrices and in measuring electrical properties of oxidized CB.[22–24]

The results on improved dispersion through functionalization of CNT as observed in TEM are in conformity with the findings of electrical property measurements.

CONCLUSIONS

NR composites compounded with both unmodified and acid-modified CNT were investigated with

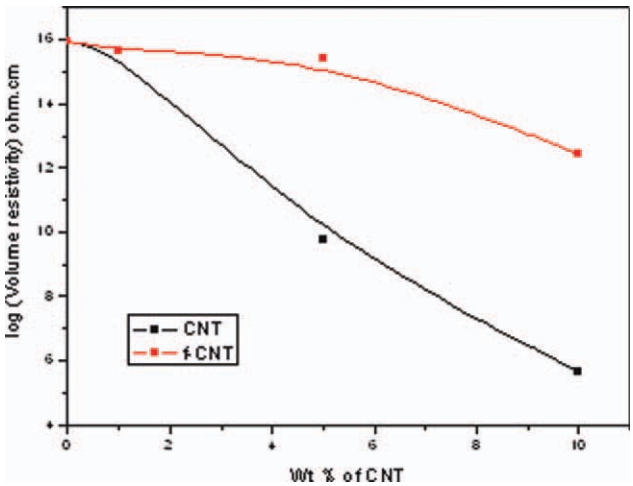

Figure 11 Volume resistivity of NR/CNT composites with (a) unmodified and (b) modified CNT. [Color figure can be viewed in the online issue, which is available at wileyonlinelibrary.com.]

respect to mechanical and dynamic mechanical properties. There is improvement in mechanical properties due to the efficient stress transfer between the matrix and filler. The dynamic mechanical properties showed enhancement especially in the low temperature region. Both storage and loss moduli showed many-fold increase for the composites with modified CNT, along with drop in the tan δ value. Crystallization of NR from DSC studies showed two different regions of crystallization due to the CNT reinforcement and coiling of NR chains over the surface of CNT. TEM studies confirm better dispersion of modified CNT in the matrix as there is drop in the aggregating tendency of CNT. In general, the acid modification of CNT improved the dynamic mechanical and mechanical properties of NR composites over a range of filler loading especially at the lower end.

References

1. Pal, P. K.; Bhowmick, A. K.; De, S. K. Rubber Chem Technol 1982, 55, 23.
2. Pal, P. K.; De, S. K. Rubber Chem Technol 1982, 55, 1370.
3. Rajeev, R. S.; De, S. K. Rubber Chem Technol 2002, 75, 475.
4. Datta, S.; Bhattacharya, A. K.; De, S. K.; Kontos, E. G.; Wefer, J. M. Polymer 1996, 37, 2581.
5. De, S. K.; White, J. R. Short Fibre-Polymer Composites; Woodhead Publishing Limited: Cambridge, 1996.
6. Nair, K. G.; Dufresne, A.; Gandini, A.; Belgace, M. N. Biomacromolecules 2003, 4, 1835.
7. Dresselhus, M. S.; Dresselhaus, G.; Eklund, P. C. Science of Fullerenes and Carbon Nanotubes; Academic Press: San Diego, 1996.
8. Swain, S. K.; Jena, I. Asian J Chem 2010, 22, 1.
9. Sahoo, N. G.; Rana, S.; Cho, J. W.; Li, L.; Chan, S. H. Prog Polym Sci 2010, 35, 837.
10. Bose, S.; Khare, R. A.; Moldenaers, P. Polymer 2010, 51, 915.
11. Kueseng, K.; Jacob, K. I. Eur Polym Mater 2006, 42, 220.
12. Lo'pez-Manchado, M. A.; Biagiotti, J.; Valentini, L.; Kenny, J. M. J Appl Polym Sci 2004, 92, 3394.
13. Kim, Y. A.; Hayashi, T.; Endo, M.; Gotoh, Y.; Wada, N.; Seiyama, J. Script Mater 2006, 54, 31.
14. Das, A.; Stöckelhuber, K.W.; Jurk, R.; Saphiannikova, M.; Fritzsche, J.; Lorenz, H.; Klüppel, M.; Heinrich, G. Polymer 2008, 49, 5276.
15. Sui, G.; Zhong, W. H.; Yang, X. P.; Yu, Y. H. Mater Sci Eng A 2008, 485, 524.
16. Das, A.; Stöckelhuber, K. W.; Jurk, R.; Heinrich, G. Macromol Symp 2010, 95, 291.
17. Socrates, G. Infrared Characteristic Group Frequencies; John Wiley & Sons, Stonebridge Press: Bristol, 1980.
18. Endo, M.; Kim, Y. A.; Fukai, Y.; Hayashi, T.; Terrones, M.; Terrons, H. Appl Phys Lett 2001, 79, 1531.
19. Bokobza, L.; Rahmani, M.; Belin, C.; Bruneel, J.; El-Bounia N. J Polym Sci B: Polym Phys 1939, 2008, 46.
20. De, S. K.; White, J. R. Rubber Technologist's Handbook; Rapra Technology Limited, Polestar Scientifica: UK, 2001.
21. Ciesielski, A. An Introduction to Rubber Technology; Smithers Rapra Technology; Redwood Books Limited: UK, 1999.
22. Blow, C. M.; Hepburn, C. Rubber Technology and Manufacture; Butterworths: London, 1982.
23. Manna, A. K.; De, P. P.; Tripathy, D. K.; De, S. K.; Chatterjee, M. K. Rubber Chem Technol 1997, 70, 624.
24. Le, H. H.; Ilisch, S.; Jakob, B.; Radusch, H.-J. Rubber Chem Technol 2004, 77, 147.